Received: 4 August 2021 | Revised: 1 September 2021 | Accepted: 28 September 2021

DOI: 10.1111/jfbc.13965

Journal of Food Biochemistry WILEY

ORIGINAL ARTICLE

Tyrosol retards induction of fibrosis in rats

Tuncer Kutlu[1] | Hüseyin Özkan[2] | Mehmet Güvenç[3]

[1]Department of Pathology, Faculty of Veterinary Medicine, Hatay Mustafa Kemal University, Hatay, Turkey

[2]Department of Genetics, Faculty of Veterinary Medicine, Hatay Mustafa Kemal University, Hatay, Turkey

[3]Department of Physiology, Faculty of Veterinary Medicine, Hatay Mustafa Kemal University, Hatay, Turkey

Correspondence
Tuncer Kutlu, Department of Pathology, Faculty of Veterinary Medicine, Hatay Mustafa Kemal University, Hatay, Turkey, 31060.
Email: tuncerkutlu83@gmail.com

Funding information
Hatay Mustafa Kemal University (Project number: 20.M.018).

Abstract

Liver fibrosis, which still does not have a standard treatment due to its complex pathogenesis, is an important cause of mortality and morbidity. In this study, it was aimed to examine the possible protective and antifibrotic effects of tyrosol on the liver through histopathologic, immunohistochemical, biochemical, and molecular methods in rats with chronic liver damage induced by thioacetamide (TAA). The study was carried out in four groups with eight rats in each group. Created groups are, respectively, control, TAA, tyrosol and TAA +tyrosol. Chronic liver damage was induced in the TAA and TAA +tyrosol groups by the addition of TAA (200 mg/L) to drinking water. Tyrosol (20 mg/kg/b.w./daily) was administered by oral gavage to tyrosol and TAA +tyrosol groups for 10 weeks. The results of this study demonstrate that the consumption of tyrosol alleviated the histopathologic changes such as inflammation, degeneration, and especially fibrosis induced by TAA in the liver. In addition, administration of tyrosol significantly attenuated alpha-smooth muscle actin (α-SMA) expression and apoptosis expression. Biochemically, it was determined that tyrosol increased glutathione (GSH) level, glutathione peroxidase (GSH.Px), and catalase (CAT) activities and showed antioxidant efficacy by reducing malondialdehyde (MDA) level. Moreover, it reduced inflammation and fibrosis by decreasing gene expression levels of tumor necrosis factor-alpha (TNF-α), interleukin-6 (IL-6), and transforming growth factor-beta (TGF-β1). Western blot analysis also revealed similar results in TGF-β1 expression. As a result, tyrosol suppressed fibrogenesis thanks to its antioxidant, anti-inflammatory, and anti-apoptotic effects and showed an antifibrotic effect in the liver.

Practical applications

It is stated that tyrosol, a natural phenolic antioxidant found in olive oil, has neuroprotective, cardioprotective, anti-inflammatory, and anticancer properties. In this study, tyrosol suppressed fibrogenesis thanks to its antioxidant, anti-inflammatory, and anti-apoptotic effects and showed an antifibrotic effect in the liver. Olive oil has an important place in the Mediterranean diet, which reduces the incidence of chronic diseases. It is thought that the anti-fibrotic effect of tyrosol plays a role in this feature. As a result, it is thought that tyrosol can be used to prevent or slow down chronic liver diseases.

KEYWORDS

apoptosis, liver fibrosis, oxidative stress, thioacetamide, tyrosol

1 | INTRODUCTION

Liver fibrosis, consequently resulting in cirrhosis, is a common pathologic consequence of liver damage, causing disability, and mortality due to liver failure (Miao et al., 2020; Sharawy et al., 2021). The liver can regenerate itself, regain its normal structure, and continue its function even in case of very severe or extensive damage. However, in recurrent chronic damages, it responds with liver fibrosis characterized by excessive extracellular matrix deposition. In this response, parenchymal cells undergo necrosis and apoptosis and the extracellular matrix (ECM) replaces these cells (Albanis & Friedman, 2006; Miao et al., 2020; Trautwein et al.; 2015). Hepatic stellate cells (HSCs) produce the majority of ECM including collagen (Albanis & Friedman, 2006; Bruck et al., 2004; Yi et al., 2015). The inflammation induced by oxidative stress plays a key role in HSC activation; HSC activation plays a pivotal role in liver fibrogenesis (Algandaby, 2018; Greenwel et al., 2000; Honda et al., 2002).

The hepatotoxin thioacetamide is an organosulfur compound with the formula of C_2H_5NS widely used to induce chronic liver damage and/or fibrosis comparable with fibrogenic changes observed in the human liver (Abramovitch et al., 2011; Algandaby, 2018; Chen et al., 2012; Müller et al., 1988; Wallace et al., 2015). Although TAA itself is not hepatotoxic, its intermediates (i.e., thioacetamide-S-oxide and thioacetamide-S,S-dioxide via the cytochrome P450) induce oxidative stress, apoptosis, necrosis, fibrosis, cirrhosis, and hepatocellular carcinoma, depending on the dose, application time, and animal species (Abramovitch et al., 2011; Müller et al., 1988; Sharawy et al., 2021; Wallace et al., 2015).

The antifibrotic effects of many bioactive constituents such as vitamin E, vitamin D, silymarin, and quercetin have been determined by in vivo and in vitro studies (Abramovitch et al., 2011; Afifi et al., 2016; Bae et al., 2018; Chen et al., 2012). The mechanisms of action of these constituents are distinctive and are in many ways such as affecting inflammation, oxidative stress, ECM production, HSC proliferation, and apoptosis (Albanis & Friedman, 2006; Bae et al., 2018). The fact that alleviating oxidative stress in the liver may have an antifibrotic effect and that antioxidants such as vitamin E can suppress fibrogenesis has been stated (Albanis & Friedman, 2006; Houglum et al., 1997; Miao et al., 2020).

Several studies have been documented that tyrosol, a natural phenolic antioxidant found in olive oil, has neuroprotective, cardioprotective, anti-inflammatory, and anticancer properties (Ahn et al., 2008; Bu et al., 2007; Chandramohan et al., 2017; Chernyshov et al., 2007; De Stefano et al., 2007; Panossian et al., 2008). In the present study, the protective effect of tyrosol on the liver and its antifibrotic effect were investigated from various aspects. Inflammatory lesions and severity of fibrosis were examined with histopathologic and immunohistochemical (α-SMA) methods. The effect of tyrosol on apoptosis was analyzed through the TUNEL (Terminal deoxynucleotidyl transferase-mediated dUTP nick end-labeling) method. Biochemically, oxidative stress parameters (GSH, GSH. Px, CAT, and MDA) were compared. In addition, mRNA and protein levels of pro-inflammatory cytokines, which are indicators of fibrosis, were examined via qPCR (TNF-α, IL-6, and TGF-β1) and western blot (TGF-β1) methods.

2 | MATERIALS AND METHODS

2.1 | Animals and experimental protocol

In this study, 32 Wistar Albino rats that are 2 months old, male, and weighing 200–250 g were used. This study was done with Hatay Mustafa Kemal University Animal Experiments Local Ethics Committee's permission numbered 2020/01-07. Rats were kept under constant environmental conditions (12 hr day/night cycles, 24 ± 3°C), received the standard commercial rat food (pellet feed), and had free access to tap water. The study was carried out in four groups with eight rats in each group. The first group was the control group and was given only 1 ml daily distilled water through oral gavage. The second group was the TAA group and 200 mg/L of TAA was added to the drinking water of rats to induce chronic liver damage (Abramovitch et al., 2011; Müller et al., 1988; Wallace et al., 2015). The third group was the tyrosol group, and tyrosol was dissolved in 1ml distilled water and administered to the rats at a dose of 20 mg/kg/b.w. daily through oral gavage for 10 weeks (Chandramohan et al., 2015). The fourth group is the TAA +tyrosol group in which tyrosol was dissolved in distilled water at a dose of 20 mg/kg/b.w. daily through oral gavage; TAA was mixed into the drinking water at a dose of 200 mg/L for the rats for 10 weeks. TAA (Sigma-Aldrich, USA, Cat no: BCCB7885) and tyrosol (Sigma-Aldrich, Cat no: 188,255) used in this study were obtained from Sigma-Aldrich. The rats were sacrificed under intraperitoneal xylazine (10 mg/kg) and ketamine (50 mg/kg) anesthesia at the end of the 10th week, and the liver tissues were removed carefully and collected for histopathologic, immunohistochemical, biochemical, and molecular tests.

2.2 | Histopathologic examination

Part of liver tissues fixed in 10% buffered formalin for 24 hr. The samples were washed under tap water, dehydrated in ascending grades of ethanol (70, 80, 90, 96, and 100%), cleared in xylene, and embedded in paraffin. Liver sections of 4 μm thickness were prepared and stained with hematoxylin and eosin (H&E) for morphologic changes, Masson's trichrome for connective tissue and Sirius red for collagen accumulation according to routine methods. After being examined under a light microscope, microphotographs were taken. Scoring of fibrosis and other histopathologic findings was made in pursuant to the Knodell Histology Activity Index (HAI) (Brunt, 2000; Knodell et al., 1981).

2.3 | Immunohistochemical examination

Avidin–biotin peroxidase complex (ABC) technique was performed according to the manufacturer guidelines (SensiTek HRP, ScyTek Laboratories, Logan, UT) to show the expression and localization of α-SMA in tissues. Paraffin-embedded liver sections were deparaffinized, hydrated, and incubated with 3% H_2O_2 to block

TABLE 1 Forward and reverse sequences of studied genes

Genes	Forward and reverse sequences	Product length	References
PPIA	F: 5′-CAGACAAAGTTCCAAAGACAGCA–3′	117	Dos Santos et al. (2016)
	R: 5′-CACCCTGGCACATGAATCCT–3′		
TNF-α	F: 5′-GGCATGGATCTCAAAGACAACC–3′	130	Castro et al. (2015)
	R: 5′-CAAATCGGCTGACGGTGTG–3′		
IL6	F: 5′-CTCTCCGCAAGAGACTTCCA–3′	92	Designed by authors
	R: 5′-TCTCCTCTCCGGACTTGTGAA–3′		
TGF-β1	F: 5′-TGACGTCACTGGAGTTGTCC–3′	141	Designed by authors
	R: 5′-CCTCGACGTTTGGGACTGAT–3′		

peroxidase activity. Proteinase K (Abcam, ab64220) was applied as antigen retrieval to the paraffin sections. Afterward, the sections were incubated with α-SMA antibody (Abcam, ab5694/1:100 dilution/45 min/45°). An endogenous avidin/biotin blocking kit (Abcam, ab64212) for endogenous biotin blocking was used. The binding sites of the antibody were visualized with 3,3′-diaminobenzidine tetrahydrochloride (DAB, ScyTek Laboratories, Logan, UT). The samples were counterstained with hematoxylin.

2.4 | Determination of apoptotic cells by TUNEL method

TUNEL method was applied in order to identify apoptotic cells in tissues. For this, In Situ Cell Death Detection and POD (Roche, Germany, Cat. No. 11,684,817,910) apoptosis kit was used and the standard prescribed procedure was applied for formalin-fixed paraffin-embedded tissues. Endogenous peroxidase activity was removed in 3% H_2O_2 methanol. Proteinase K (Abcam, ab64220) was used as an antigen retrieval and DAB (ScyTek Laboratories, Logan, UT) was used as a chromogen. TUNEL and α-SMA activities in tissues were scored semi-quantitatively as negative (0), mild (1), moderate (2), and severe (3) under a light microscope (Kutlu & Alcigir, 2019; Sen et al., 2017; Sharawy et al., 2021).

2.5 | Biochemical examination

After the tissues were taken for lipid peroxidation and antioxidant activity are homogenized; analyses were conducted with the help of a spectrophotometer. The level of lipid peroxidation was measured relative to the concentration of thiobarbituric acid reagents, and the amount of MDA produced was used as an index of lipid peroxidation. At 532 nm, the MDA level was expressed in nanomoles per gram of protein (Placer et al., 1966). GSH level was measured by using the method defined by Sedlak and Lindsay (1968). The GSH level at 412 nm was expressed as nanomoles per gram of protein. The glutathione peroxidase (GSH-Px, EC 1.11.1.9) activity was determined via the method defined by Lawrence and Burk (1976). GSH. Px activity at 340 nm was expressed by international units per gram of protein. Catalase activity (EC 1.11.1.6) was determined by measuring hydrogen peroxide decomposition at 240 nm and expressed as kg/protein (Aebi, 1983). The Lowry method was used for protein analysis (Lowry et al., 1951).

2.6 | Molecular examination

Samples were quickly frozen in liquid nitrogen after euthanasia were stored at −86°C until RNA isolation. Approximately 50 mg from each sample was taken and homogenized in 1 mL Tri-Reagent with a homogenizer (DAIHAN Scientific HG-15D). Total RNA was isolated according to the TRI-Reagent kit (Sigma-Aldrich, Cat. no: T9424) protocol (Rio et al., 2010). For this purpose, RNA pellets were obtained after chloroform-isopropyl alcohol-ethyl alcohol processes from the samples kept in Tri-Reagent for about 10 min at room temperature. Obtained RNA pellets were dissolved with 30–100 μL nuclease-free water depending on their size. The purity (A260/280) and concentration values of the RNAs isolated from the samples were checked on the nucleic acid meter (SMA-1000 UV Spectrophotometer). In addition, RNA quality was assessed over 28S and 18S rRNA subunits in 1% agarose gel (100 V and 25 min). Before cDNA synthesis, possible genomic DNAs were removed from samples that proper purity, concentration, and integrity with DNA digestion kit (DNase I, RNase free, Thermo Scientific, USA, Cat no: EN0525). cDNA synthesis was performed at 25°C for 10 min, at 37°C for 120 min, and at 85°C for 5 min, in accordance with the High Capacity cDNA Reverse Transcription kit protocol (Thermo-Fisher Scientific, Cat. no: 4,368,814) in a thermal cycler (Biorad T100, USA). The final volume of the samples after the reaction was completed to 200 μl and stored at −80°C until gene expression studies were performed. Amplification of the target genes was performed via a kit containing SYBR Green I dye by using 10 μL of each cDNA sample (Power SYBR® Green PCR Master, Thermo-Fisher Scientific, Cat no: 4,367,659). Each sample was studied as a duplicate. In real-time PCR (Bio-Rad CFX-96 Touch Real Time PCR, USA), the reaction was arranged as 10 min at 95°C, followed by 15 s at 95°C, 60 s at 60°C, and 40 cycles. PPIA (Peptidyl-Prolyl Cis-Trans Isomerase A) gene was used as a housekeeping gene. The forward and reverse primer sequences used in the amplification of genes are given in Table 1.

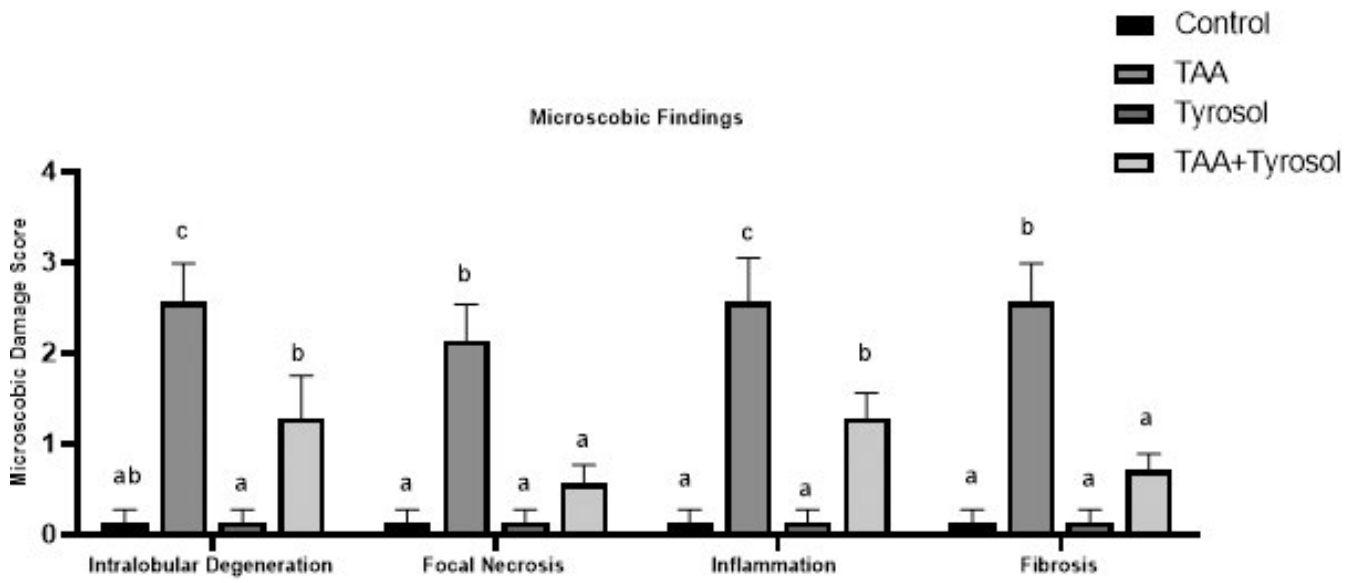

FIGURE 1 Histopathologic findings and scoring were observed in the groups. Data are expressed as mean ± *SEM*. Different superscript letters (a, b, c) within the same column show statistically significant differences between the groups ($p < .001$)

2.7 | Western blot analysis

After the tissues were homogenized through cold RIPA lysis buffer (sc-24948A) according to the protocol, they were centrifuged at +4° at 14,000 rpm and the supernatant liquid was separated. The total amount of protein in the samples was determined spectrophotometrically by using BCA (Smith et al., 1985) in accordance with the protocol (Pierce™ BCA Protein Assay Kit). Samples were loaded onto polyacrylamide gel in equal amounts of protein (40 μg) in each well and electrophoresed (Laemmli, 1970), and after SDS-PAGE, proteins were transferred to polyvinylidene difluoride (PVDF) membrane by the western blotting technique (Towbin et al., 1979). After this process, PVDF membranes were blocked with 5% milk powder in order to prevent nonspecific binding and washed with TBS-T three times for 5 min each. After diluting the membranes with TGF-Beta (CST 5,544, rabbit polyclonal antibody, 1/1,000), beta-actin (CST 4,970, rabbit monoclonal antibody, 1/5,000) antibodies using 5% milk powder according to the protocol, then they were left to incubate overnight, and after the incubation, the membranes were washed with TBS-T three times for 5 min each. After the secondary antibodies (CST 7,074 1/2,000) were diluted with 5% milk powder, the membranes were incubated for 1 hr with secondary antibodies. After the incubation, the membranes were washed again with TBS-T for 5 min three times, and the bands obtained by using chemiluminescent conjugate (ECL; Biorad 1,705,061) were monitored in the chemiluminescence imaging (Biorad ChemiDoc™ MP) (Bass et al., 2017; Sambrook et al., 1989). The band intensities in the images obtained were measured with a proper analysis system (Biorad Image Lab TM Software, version 5.2.1, Biorad Laboratories, Inc., USA). The data were normalized in accordance with beta-actin used as an internal control and expressed as a percentage of the control.

2.8 | Statistical analysis

Shapiro-Wilk normality analysis was performed on the data gathered at the end of the study in order to determine whether the values regarding the groups present normal distribution and at the end of the test it was revealed that the values in all parameters exhibited normal distribution. One-way analysis of variance (ANOVA) was used to compare group averages, and the Tukey test was used to determine differences between groups. Statistical assessment was carried out using IBM SPSS Statistics, v.23 software, and $p < .05$ value was considered to be statistically significant. In the assessment of gene expression analysis, the results were given as fold-change by using the $2^{-\Delta\Delta Ct}$ method and compared with the control group (Livak & Schmittgen, 2001).

3 | RESULTS

Macroscopically, in the control and tyrosol groups, livers were reddish in color and no lesions were observed. It was found that the liver of animals in TAA and TAA +tyrosol groups was whitish in color, much more in the TAA group; reddish foci with distinct borders were observed on the surface.

Microscopically, histopathologic findings and scoring observed in the groups are summarized in Figure 1 ($p < .001$). Histopathologic findings scoring was performed according to Knodell Histologic Activity Index (HAI). Masson's trichrome and Sirius red staining were performed to examine the degree of connective tissue and collagen accumulation. In the control and tyrosol groups, rats showed normal hepatic parenchyma with normally arranged hepatic cords (Figures 2a and 3a,b). In the TAA group, the vessels were hyperemic, there were changes ranging from degeneration to necrosis in

hepatocytes. Diffuse Kupffer cell proliferation among hepatocytes, focal inflammatory cell infiltration especially in the portal regions, disorganization of hepatic cords, anisokaryosis of hepatocytes, and biliary hyperplasia were found. In addition, different degrees of hepatocellular proliferation, increase in connective tissue extending to the portal region or central septa, collagen accumulation, and regenerating hepatic nodule were observed (Figures 2b–d, 3c). The TAA +tyrosol group showed improvement in hepatic architecture, but still has lesions, statistically, significantly less degeneration, necrosis, fibrosis, and inflammatory cell infiltration were observed. Regenerating hepatic nodule was not observed (Figure 2e,f). It was noted that collagen accumulation was less in this group than in the TAA group (Figure 3d).

In the α-SMA staining performed for the detection of active HSCs, positivity was observed only in the vessel walls in the control and tyrosol groups (Figure 4a). In the TAA group, positivity was found to be strong and widespread, especially in portal regions, together with positivity in the vessels (Figure 4b,c). However, in the TAA +tyrosol group, there were also mild positive foci in the portal area (Figure 4d). Although there were mild expressions in hepatocytes in the control and tyrosol groups in the TUNEL staining performed for apoptosis, there was a very strong positivity in the hepatocytes in the TAA group (Figure 4e–g). It was milder in the TAA group than it was in the TAA +Tyrosol group (Figure 4h). Expression scoring for α-SMA and apoptosis are presented in Figure 5 ($p < .001$).

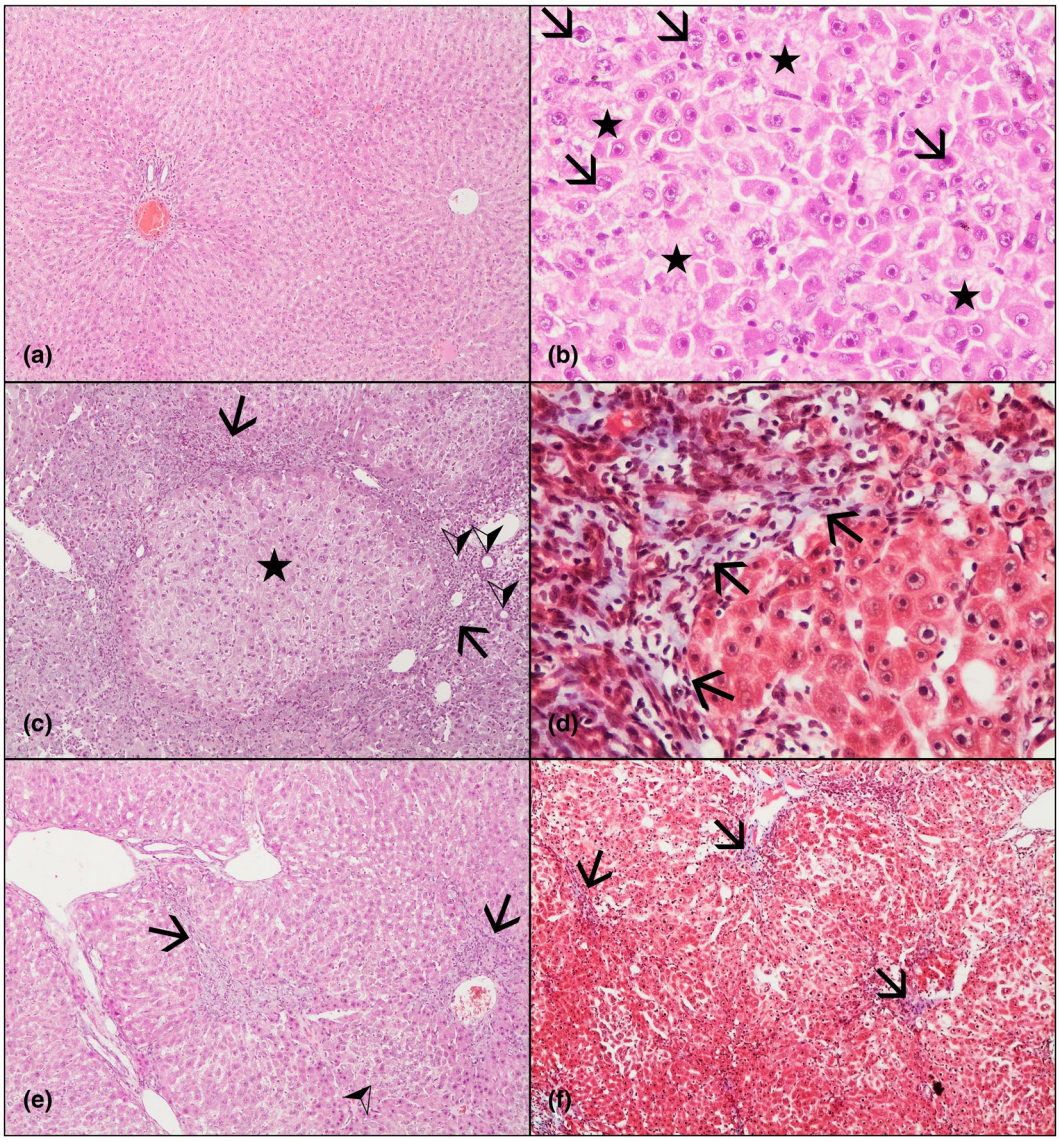

FIGURE 2 Histopathologic appearance of liver a) Control: normal liver tissue histology. H&E. 100×. b) TAA: degenerative and necrotic changes in hepatocytes (stars) and anisonucleosis of hepatocytes (arrows). H&E. 400×. c) TAA: regenerating hepatic nodule (star), biliary hyperplasia (arrowheads), mononuclear cells infiltration, and fibrosis (arrows). H&E. 100×. d) TAA: connective tissue increase in the portal area (arrows), Masson's trichrome stain, 400×. e) TAA +tyrosol: mild connective tissue increase and inflammatory cell infiltration, H&E. 100×. f) TAA +tyrosol: mild connective tissue increase and inflammatory cell infiltration, Masson's trichrome stain. 100×

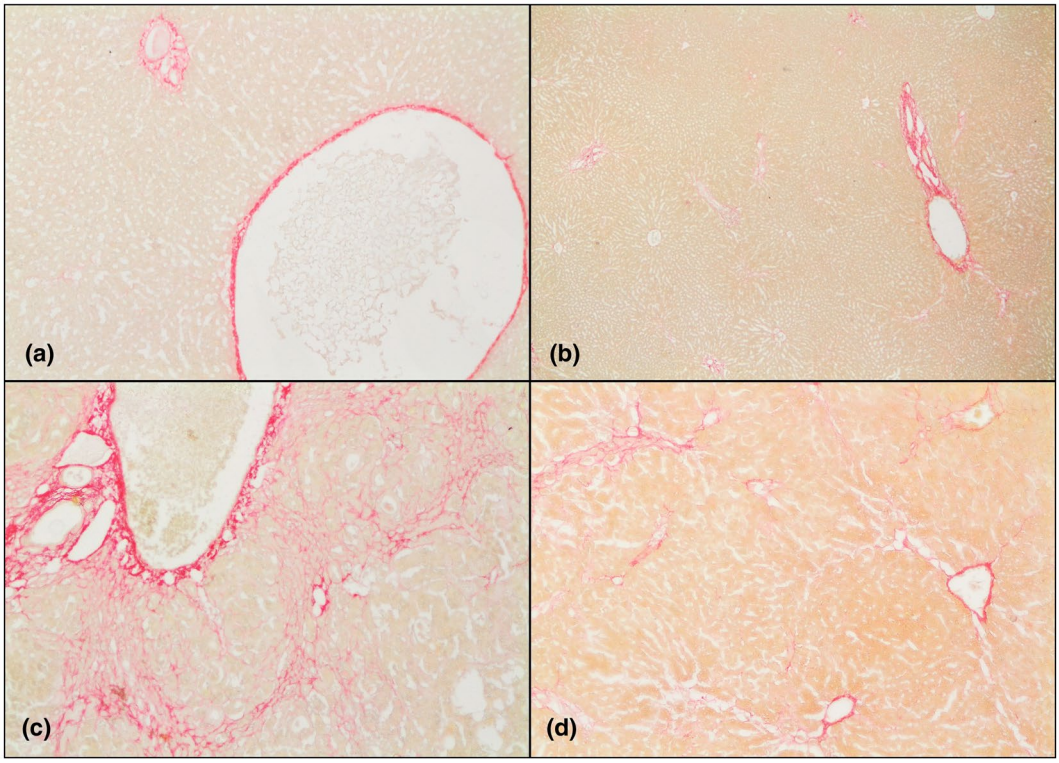

FIGURE 3 Collagen accumulation in the liver a) Control: collagen in the vascular wall, Sirius red stain. 100×. b) Tyrosol: collagen in the vascular wall, Sirius red stain. 100×, c) TAA: collagen in the vascular wall and in portal areas intensively, Sirius red stain, 100×. d) TAA +tyrosol: collagen in the vascular wall and in portal areas weakly, Sirius red stain, 100×

The oxidative stress and antioxidant efficacy markers obtained at the end of the study are given in Figure 6. It was determined that the MDA levels in the TAA group showed a significant increase compared with the control group; however, the MDA levels in the TAA +tyrosol and tyrosol groups were close to the control group. The GSH level used for antioxidant efficacy and the GSH. Px and CAT activities were significantly decreased in the TAA group compared with the control group and a significant increase in the tyrosol group. In the TAA +tyrosol group, a significant increase was detected in GSH and GSH. Px and CAT levels compared with the TAA group, and CAT activity was found to be at the control group's level. The data obtained at the end of the study through western blot analysis are given in Figure 7. TGF-β expression was observed to be lesser in the tyrosol group compared with the control group. In the TAA +tyrosol group, on the other hand, the increase in TGF-β expression was found to be significantly less compared with the TAA group.

The isolated RNAs were determined to be appropriate in terms of purity and concentration. Expression levels of the target genes (TNF-α, IL-6, and TGF-β1) are given in Figure 7. TNF-α gene expression was twice as high in the TAA group compared with the control group; tyrosol and TAA +tyrosol groups were observed to be below the control group. Similarly, IL-6 expression in the TAA group was approximately fivefold higher compared with the control group and approximately twofold higher than TAA +tyrosol group. In the tyrosol group, it was below the control group. TGF-β1 expression was observed to be 2.21 in the TAA group, 1.40 in the tyrosol group, and 1.52 in the TAA +tyrosol group.

4 | DISCUSSION

In recurrent chronic damages in the liver, liver fibrosis is characterized through inflammatory cell infiltration and accumulation of excess extracellular matrix (Albanis & Friedman, 2006; Trautwein et al., 2015). Thioacetamide, which is widely used in the induction of experimental chronic liver damage and fibrosis, causes oxidative stress and centrilobular necrosis (Abramovitch et al., 2011; Mansour et al., 2018; Müller et al., 1988; Wallace et al., 2015). In a study conducted on mice, it was reported that TAA increases TNF-α and IL-6 mRNA levels, lowers the GSH. Px level, and causes necrosis and inflammation. It has been stated that these changes occur after increased oxidative stress (Kang et al., 2008; Sanchez-Valle et al., 2012). In the present study, it was determined that the mixing of TAA to drinking water caused oxidative stress, inflammation, and consequently liver fibrosis.

In this study, when TAA was mixed into the drinking water of rats at a dose of 200 mg/L for 10 weeks, it caused morphologic changes, such as degeneration, inflammation, biliary hyperplasia, necrosis, and fibrosis, similar to previous studies (Abramovitch et al., 2011; Afifi et al., 2016; Czechowska et al., 2015; El-Baz et al., 2019; Mansour et al., 2018; Müller et al., 1988; Wallace et al., 2015). When rats consumed TAA and tyrosol together, it was observed that morphologic changes, especially

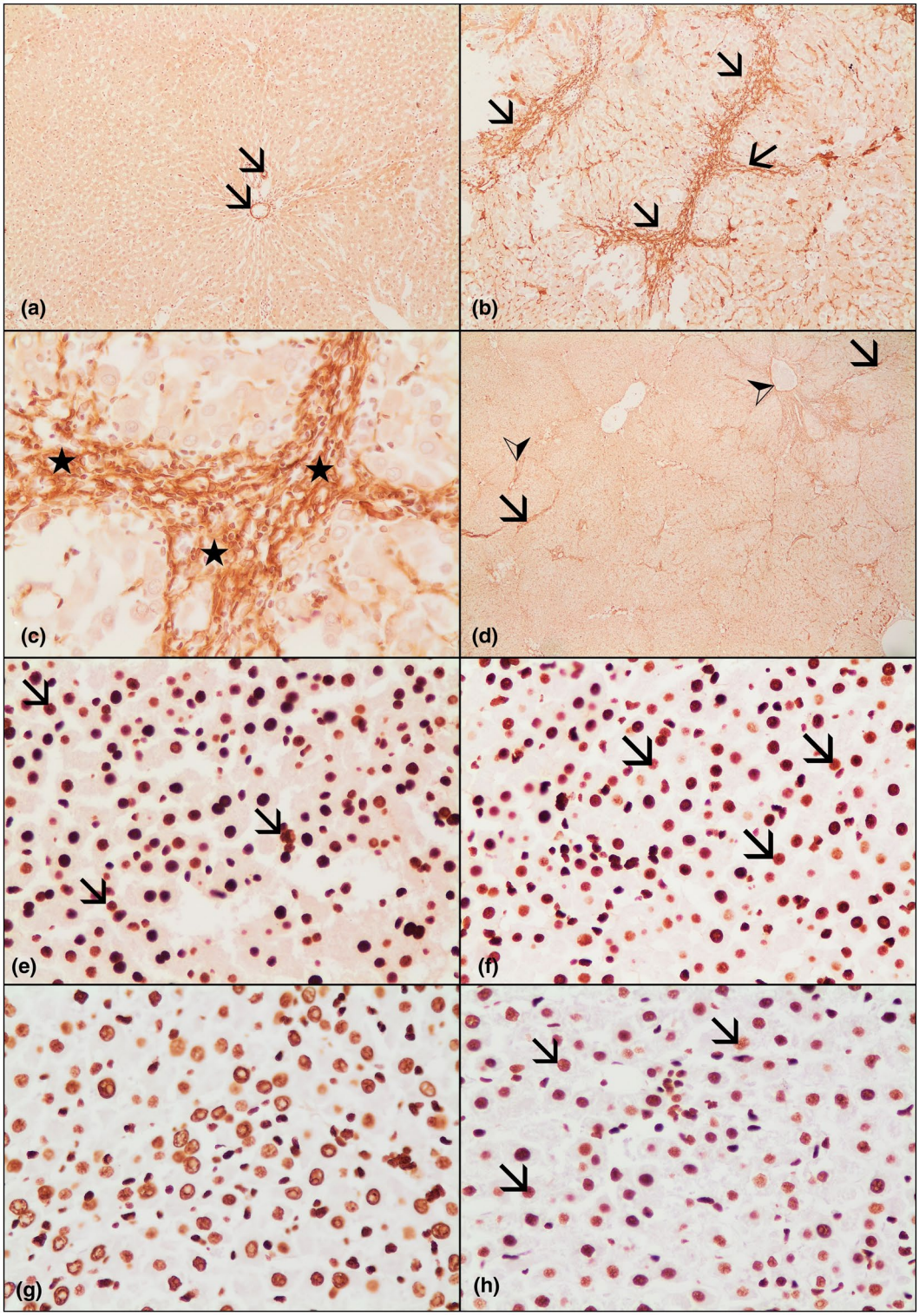

FIGURE 4 Immunohistochemical staining for α-SMA demonstrating activated HSCs and TUNEL staining for demonstrating apoptotic cells. a) Control: no positive immunostaining for α-SMA except vascular wall (arrows), 100×. b) TAA: strong positivity for α-SMA especially in portal areas (arrows), 100×. c) TAA: strong positivity for α-SMA especially in portal areas (star), 400×. d) TAA +tyrosol: mild positivity for α-SMA especially in portal areas (star), 100×. e) Control: mild TUNEL-positive apoptotic hepatocytes (arrows), 400×. f) Tyrosol: mild TUNEL-positive apoptotic hepatocytes (arrows), 400×. g) TAA: strong TUNEL-positive apoptotic hepatocytes (arrows), 400×. h) TAA +tyrosol: mild TUNEL-positive apoptotic hepatocytes (arrows), 400×

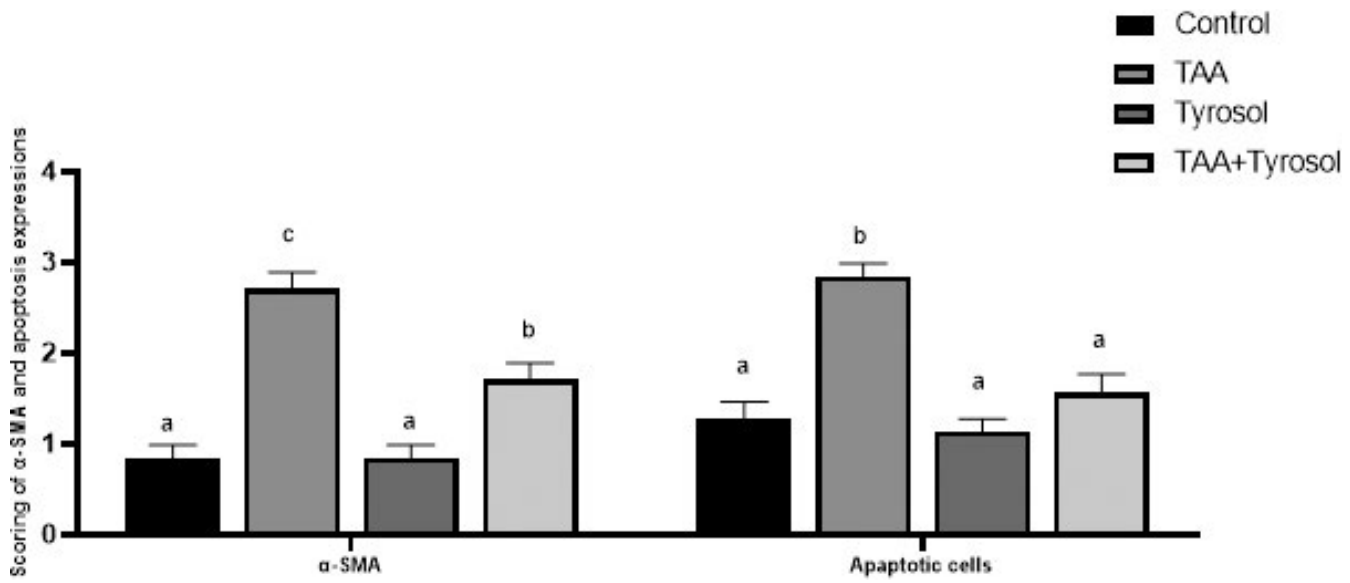

FIGURE 5 Expression scoring for α-SMA and apoptosis. Data are expressed as mean ± *SEM*. Different superscript letters (a, b, c) within the same column show statistically significant differences between the groups ($p < .001$)

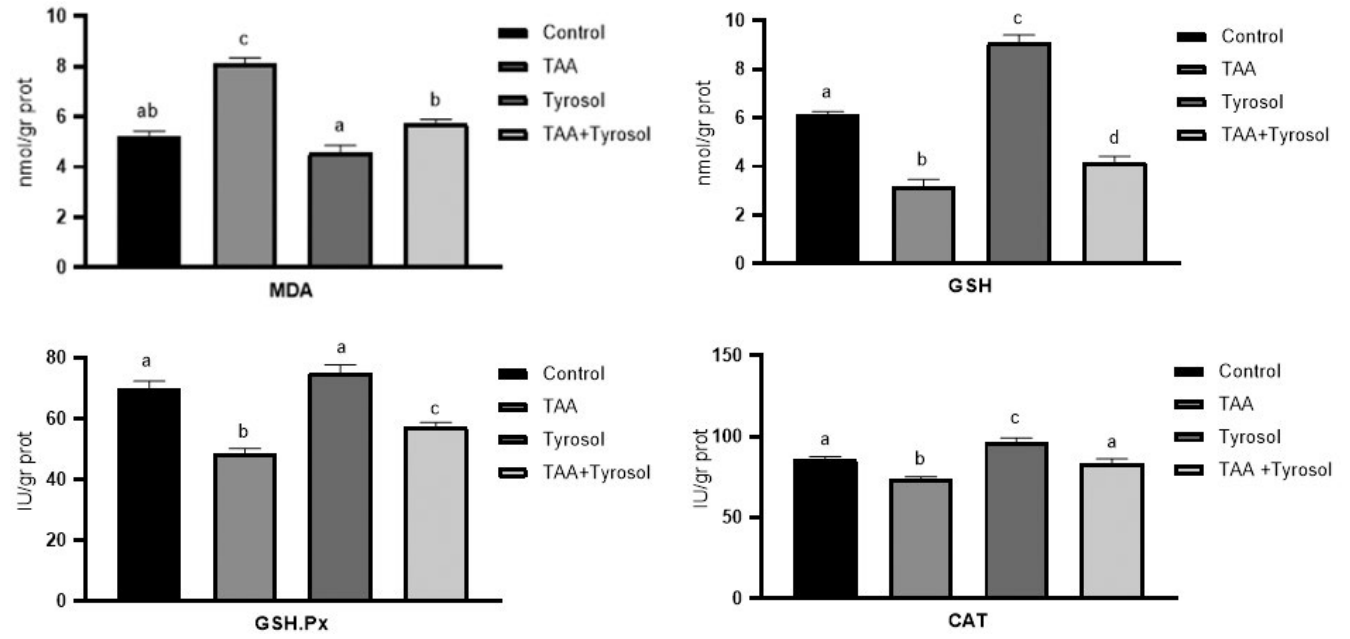

FIGURE 6 MDA, GSH, GSH. Px, and CAT levels in liver tissues of different groups. Data are expressed as mean ± *SEM*. Different superscript letters (a, b, c) within the same column show statistically significant differences between the groups ($p < .001$)

fibrosis, were markedly alleviated. It has been reported that substances such as melatonin, silymarin, crocin, tadalafil, vitamin D, and benzoquinone have similar effects, reducing the morphologic changes caused by TAA (Abramovitch et al., 2011; Algandaby, 2018; Chen et al., 2012; Czechowska et al., 2015; Mansour et al., 2018; Miao et al., 2020).

The progression of fibrogenesis increases collagen synthesis and collagen increase is accepted as a marker of fibrosis (El-Baz et al., 2019). The majority of ECM, including collagen, is produced by active HSCs that play a pivotal role in fibrogenesis (Honda et al., 2002; Iredale et al., 1998). In vivo HSC activation is a complex process in which growth factors, cytokines, chemokines, and oxidative stress products, play a key role (Palacios et al., 2008). The inflammation induced by oxidative stress causes necrosis and apoptosis in hepatocytes, initiating HSC activation, and fibrogenesis (Algandaby et al., 2018; Greenwel et al., 2000; Mansour et al., 2018). Activation of HSCs and their differentiation into myofibroblast-like cells cause ECM increase and α-SMA expression (El-Baz et al., 2019; Mansour et al., 2018; Sharawy et al., 2021). In the present study,

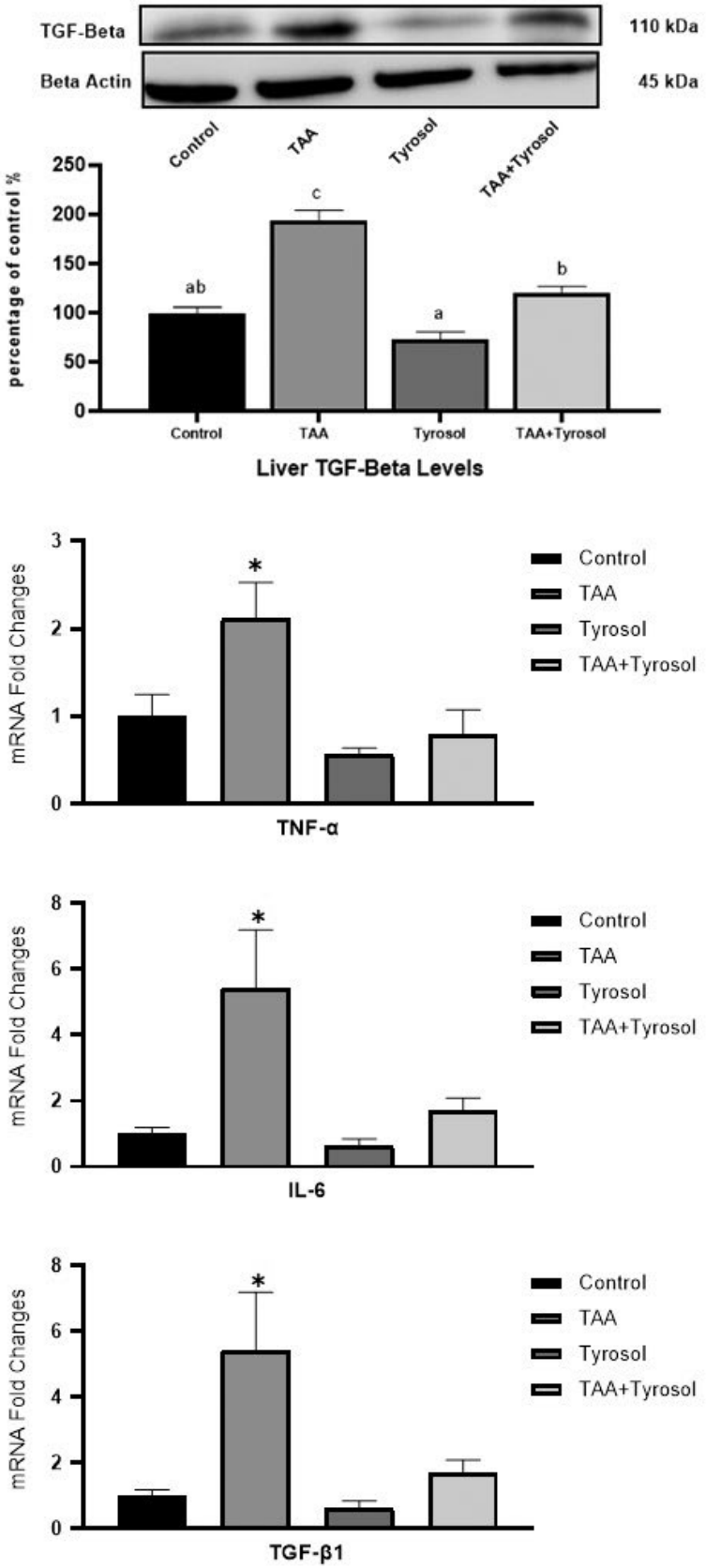

FIGURE 7 Effect of tyrosol on western blot analysis of TGF-Beta in the liver tissue of control and experimental rats. Protein expression is normalized to β-actin. Data are shown as percent of control. Representative western blot picture of TGF-Beta and Beta Actin in the liver. Mean TGF-Beta expression levels (%) Data are expressed as mean ± *SEM*. Different superscript letters (a, b, c) within the column show statistically significant differences between the groups ($p < .001$) and gene expression results of TNF-α, IL-6, and TGF-β1 in the liver. Fold change differences in groups were compared with control. Results were presented as mean ± *SEM*, $^{*}p < .05$

while TAA increased hepatic collagen content and α-SMA expression, it was found that tyrosol decreased the amount of collagen and α-SMA expression. It was reported that substances such as *D. salina*, paclitaxel, and silymarin showed similar effects in rats and decreased α-SMA positivity and collagen amount (Chen et al., 2012; El-Baz et al., 2019; Mansour et al., 2018; Sharawy et al., 2021).

Afifi et al. (2016) reported that TAA causes hepatocellular apoptosis, but quercetin inhibits apoptosis. In the current study, in TUNEL staining performed for the detection of apoptosis, it was found that TAA stimulated apoptosis but tyrosol suppressed it. Stiuso et al. (2016) stated that tyrosol protected the liver by inhibiting apoptosis in their in vitro study. Kalaiselvan et al. (2016) on the other hand, in their in vivo studies, associated the antiapoptotic property of tyrosol with the decrease of proapoptotic Bax protein expression and the increase of anti-apoptotic Bcl-2 protein expression.

In previous studies, it was determined that TAA causes oxidative stress by decreasing the amount of glutathione and increasing the ROS-induced lipid peroxidase levels (Abramovitch et al., 2011; Afifi et al., 2016; Müller et al., 1988; Wallace et al., 2015). These free radicals affect hepatocytes, endothelial cells, Kupffer cells, and HSCs by inducing inflammation, ischemia, apoptosis, necrosis, and regeneration (Sánchez-Valle et al., 2012). In this study, it was found that TAA increases the MDA level, and it decreases GSH, GSH. Px, and CAT levels. Earlier studies showed that this oxidative stress caused by TAA decreased with tyrosol. In other studies, it has been reported that tyrosol has a protective effect on the liver by reducing oxidative stress in hepatocytes (Armutcu et al., 2013; Kalaiselvan et al., 2016; Roche et al., 2009; Sarna et al., 2016). Sarna et al. (2016) determined that tyrosol exhibits this protective activity by increasing cystathionine β-synthase and cystathionine γ-lyase expression and endogenous hydrogen sulfide synthesis in the liver.

In clinical and experimental studies, the formation of ROS and oxidative stress plays an important role in initiating hepatic fibrogenesis, and it has been stated that oxidative stress initiates fibrosis by increasing the inflammatory reaction and the release of profibrogenic mediators (Mansour et al., 2018; Sánchez-Valle et al., 2012). Parallelism was found between the expression levels of TNF-α, IL-6, and TGF-β1 cytokines involved in fibrogenesis with HSC activation and transdifferentiation in TAA-induced fibrogenesis (Palacios et al., 2008). It has been reported that TAA application initiates inflammation by increasing serum levels of TNF-α, IL-6, and TGF-pro1 pro-inflammatory cytokines in rats compared with the control group (Czechowska et al., 2015; El-Baz et al., 2019; Mansour et al., 2018).

In the present study, it was determined that TAA increased gene expression levels of TNFα, IL-6, TGF-β1 cytokines related to inflammation, and fibrosis together with oxidative stress in liver disease. It was determined that tyrosol reduced the oxidative stress caused by TAA as well as reducing the gene expression of these cytokines and showing anti-inflammatory and antifibrotic effects. Substances such as melatonin, silymarin, crocin, quercetin, and tadalafil have also been found to reduce the expression of TNF-α, IL-6, and TGF-β1 in TAA-induced fibrosis (Afifi et al., 2016; Algandaby et al., 2018; Chen et al., 2012; Czechowska et al., 2015; Mansour et al., 2018). It has also been reported in previous in vivo studies that tyrosol has an anti-inflammatory effect (Armutcu et al., 2013; Chandramohan et al., 2017; Roche et al., 2009).

In conclusion, in this study, tyrosol exhibited its hepatoprotective effect with different mechanisms and showed an anti-fibrotic effect on reducing oxidative stress caused by TAA, by inhibiting fibrosis-related cytokines and reducing apoptosis.

ACKNOWLEDGMENT

This study was financially supported by the Scientific Research Projects Coordination of Hatay Mustafa Kemal University (Project number: 20.M.018).

CONFLICT OF INTEREST

The authors declare that they have no conflict of interest.

AUTHOR CONTRIBUTION

Tuncer Kutlu: Investigation; Methodology; Project administration; Resources; Supervision; Visualization; Writing-review & editing. **Huseyin Ozkan:** Investigation; Methodology; Writing-original draft. **Mehmet Guvenc:** Investigation; Methodology; Writing-review & editing.

ORCID

Tuncer Kutlu https://orcid.org/0000-0002-8771-1256

REFERENCES

Abramovitch, S., Dahan-Bachar, L., Sharvit, E., Weisman, Y., Tov, A. B., Brazowski, E., & Reif, S. (2011). Vitamin D inhibits proliferation and profibrotic marker expression in hepatic stellate cells and decreases thioacetamide-induced liver fibrosis in rats. *Hepatology*, *60*(12), 1728–1737.

Aebi, H. Catalase. In H. U. Bergmeyer (Ed.), *Methods of enzymatic analysis* (pp. 273–286). Verlag Chemie; 1983.

Afifi, N. A., Ramadan, A., El-Eraky, W., Salama, A. A. A., El-Fadaly, A. A., & Hassan, A. (2016). Quercetin protects against thioacetamide induced hepatotoxicity in rats through decreased oxidative stress biomarkers, the inflammatory cytokines;(TNF-α),(NF-κ B) and DNA fragmentation. *Der Pharma Chemica*, *8*(9), 48–55.

Ahn, E. Y., Jiang, Y., Zhang, Y., Son, E. M., You, S., Kang, S. W., Park, J. S., Jung, J. H., Lee, B. J., & Kim, D. K. (2008). Cytotoxicity of p-tyrosol and its derivatives may correlate with the inhibition of DNA replication initiation. *Oncology Reports*, *19*, 527–534. https://doi.org/10.3892/or.19.2.527

Albanis, E., & Friedman, S. L. (2006). Antifibrotic agents for liver disease. *American Journal of Transplantation*, *6*(1), 12–19. https://doi.org/10.1111/j.1600-6143.2005.01143.x

Algandaby, M. M. (2018). Antifibrotic effects of crocin on thioacetamide-induced liver fibrosis in mice. *Saudi Journal of Biological Sciences*, *25*(4), 747–754. https://doi.org/10.1016/j.sjbs.2016.10.007

Armutcu, F., Namuslu, M., Yüksel, R., & Kaya, M. (2013). Zeytinyağı ve sağlık: Biyoaktif bileşenleri, antioksidan özellikleri ve klinik etkileri. *Konuralp Tıp Dergisi*, *5*(1), 60–68.

Bae, M., Park, Y. K., & Lee, J. Y. (2018). Food components with antifibrotic activity and implications in prevention of liver disease. *Journal of Nutritional Biochemistry*, *55*, 1–11. https://doi.org/10.1016/j.jnutbio.2017.11.003

Bass, J. J., Wilkinson, D. J., Rankin, D., Phillips, B. E., Szewczyk, N. J., Smith, K., & Atherton, P. J. (2017). An overview of technical considerations for Western blotting applications to physiological research. *Scandinavian Journal of Medicine and Science in Sports*, *27*(1), 4–25. https://doi.org/10.1111/sms.12702

Bruck, R., Schey, R., Aeed, H., Hochman, A., Genina, O., & Pines, M. (2004). A protective effect of pyrrolidine dithiocarbamate in a rat model of liver cirrhosis. *Liver International: Official Journal of the International Association for the Study of the Liver*, *24*(2), 169–176. https://doi.org/10.1111/j.1478-3231.2004.00900.x

Brunt, E. M. (2000). Grading and staging the histopathological lesions of chronic hepatitis: The Knodell histology activity index and beyond. *Hepatology*, *31*(1), 241–246. https://doi.org/10.1002/hep.510310136

Bu, Y., Rho, S., Kim, J., Kim, M. Y., Lee, D. H., Kim, S. Y., Choi, H., & Kim, H. (2007). Neuroprotective effect of tyrosol on transient focal cerebral ischemia in rats. *Neuroscience Letters*, *414*, 218–221. https://doi.org/10.1016/j.neulet.2006.08.094

Castro, M. C., Massa, M. L., Arbeláez, L. G., Schinella, G., Gagliardino, J. J., & Francini, F. (2015). Fructose-induced inflammation, insulin resistance and oxidative stress: A liver pathological triad effectively disrupted by lipoic acid. *Life Sciences*, *137*, 1–6. https://doi.org/10.1016/j.lfs.2015.07.010

Chandramohan, R., Pari, L., Rathinam, A., & Sheikh, B. A. (2015). Tyrosol, a phenolic compound, ameliorates hyperglycemia by regulating key enzymes of carbohydrate metabolism in streptozotocin induced diabetic rats. *Chemico-Biological Interactions*, *229*, 44–54. https://doi.org/10.1016/j.cbi.2015.01.026

Chandramohan, R., Saravanan, S., & Pari, L. (2017). Beneficial effects of tyrosol on altered glycoprotein components in streptozotocin-induced diabetic rats. *Pharmaceutical Biology*, *55*(1), 1631–1637. https://doi.org/10.1080/13880209.2017.1315603

Chen, I. S., Chen, Y. C., Chou, C. H., Chuang, R. F., Sheen, L. Y., & Chiu, C. H. (2012). Hepatoprotection of silymarin against thioacetamide-induced chronic liver fibrosis. *Journal of the Science of Food and Agriculture*, *92*(7), 1441–1447. https://doi.org/10.1002/jsfa.4723

Chernyshov, G. A., Plotnikov, M. B., Smol′iakova, V. I., & Krasnov, E. A. (2007). Therapeutic effect of p-tyrosol on myocardial electric instability induced by coronary occlusion. *Eksperimentalnaia I Klinicheskaia Farmakologiia*, *70*, 23–25.

Czechowska, G., Celinski, K., Korolczuk, A., Wojcicka, G., Dudka, J., Bojarska, A., & Reiter, R. J. (2015). Protective effects of melatonin against thioacetamide-induced liver fibrosis in rats. *Journal of Physiology and Pharmacology*, *66*(4), 567–579.

De Stefano, D., Maiuri, M. C., Simeon, V., Grassia, G., Soscia, A., Cinelli, M. P., & Carnuccio, R. (2007). Lycopene, quercetin and tyrosol prevent macrophage activation induced by gliadin and IFN-gamma. *European Journal of Pharmacology*, *566*, 192–199.

dos Santos, B. P., da Costa Diesel, L. F., da Silva, M. L., Nardi, N. B., & Camassola, M. (2016). Identification of suitable reference genes for quantitative gene expression analysis in rat adipose stromal cells induced to trilineage differentiation. *Gene*, *594*(2), 211–219. https://doi.org/10.1016/j.gene.2016.09.002

El-Baz, F. K., Salama, A., & Salama, R. A. (2019). Therapeutic effect of Dunaliella salina microalgae on thioacetamide-(TAA-) induced hepatic liver fibrosis in rats: Role of TGF-β and MMP9. *BioMed Research International*, 1–9.

Greenwel, P., Domínguez-Rosales, J. A., Mavi, G., Rivas-Estilla, A. M., & Rojkind, M. (2000). Hydrogen peroxide: A link between acetaldehyde-elicited α1 (i) collagen gene up-regulation and oxidative stress in mouse hepatic stellate cells. *Hepatology*, *31*(1), 109–116. https://doi.org/10.1002/hep.510310118

Honda, H., Ikejima, K., Hirose, M., Yoshikawa, M., Lang, T., Enomoto, N., Kitamura, T., Takei, Y., & Sato, N. (2002). Leptin is required for fibrogenic responses induced by thioacetamide in the murine liver. *Hepatology*, *36*(1), 12–21. https://doi.org/10.1053/jhep.2002.33684

Houglum, K., Venkataramani, A., Lyche, K., & Chojkier, M. (1997). A pilot study of the effects of d-alpha-tocopherol on hepatic stellate cell activation in chronic hepatitis C. *Gastroenterology*, *113*(4), 1069–1073. https://doi.org/10.1053/gast.1997.v113.pm9322499

Iredale, J. P., Benyon, R. C., Pickering, J., McCullen, M., Northrop, M., Pawley, S., Howel, C., & Arthur, M. J. (1998). Mechanisms of spontaneous resolution of rat liver fibrosis. Hepatic stellate cell apoptosis and reduced hepatic expression of metalloproteinase inhibitors. *Journal of Clinical Investigation*, *102*(3), 538–549. https://doi.org/10.1172/JCI1018

Kalaiselvan, I., Samuthirapandi, M., Govindaraju, A., Sheeja Malar, D., & Kasi, P. D. (2016). Olive oil and its phenolic compounds (hydroxytyrosol and tyrosol) ameliorated TCDD-induced heptotoxicity in rats via inhibition of oxidative stress and apoptosis. *Pharmaceutical Biology*, *54*(2), 338–346. https://doi.org/10.3109/13880209.2015.1042980

Kang, J. S., Wanibuchi, H., Morimura, K., Wongpoomchai, R., Chusiri, Y., Gonzalez, F. J., & Fukushima, S. (2008). Role of CYP2E1 in thioacetamide-induced mouse hepatotoxicity. *Toxicology and Applied Pharmacology*, *228*(3), 295–300. https://doi.org/10.1016/j.taap.2007.11.010

Knodell, R. G., Ishak, K. G., Black, W. C., Chen, T. S., Craig, R., Kaplowitz, N., Kiernan, T. W., & Wollman, J. (1981). Formulation and application of a numerical scoring system for assessing histological activity in asymptomatic chronic active hepatitis. *Hepatology*, *1*, 431–435. https://doi.org/10.1002/hep.1840010511

Kutlu, T., & Alcigir, G. (2019). Comparison of renal lesions in cats and dogs using pathomorphological and ımmunohistochemical methods. *Biotechnic and Histochemistry*, *94*(2), 126–133. https://doi.org/10.1080/10520295.2018.1522670

Laemmli, U. K. (1970). Cleavage of structural proteins during the assembly of the head of bacteriophage T4. *Nature*, *227*(5259), 680–685. https://doi.org/10.1038/227680a0

Lawrence, R. A., & Burk, R. F. (1976). Glutathione peroxidase activity in selenium-deficient rat liver. *Biochemical and Biophysical Research Communications*, *71*(4), 952–958. https://doi.org/10.1016/0006-291X(76)90747-6

Livak, K. J., & Schmittgen, T. D. (2001). Analysis of relative gene expression data using real-time quantitative PCR and the 2− ΔΔCT method. *Methods*, *25*(4), 402–408. https://doi.org/10.1006/meth.2001.1262

Lowry, O. H., Rosebrough, N. J., Farr, A. L., & Randall, R. J. (1951). Protein measurement with the Folin phenol reagent. *Journal of Biological Chemistry*, *193*, 265–275. https://doi.org/10.1016/S0021-9258(19)52451-6

Mansour, H. M., Salama, A. A., Abdel-Salam, R. M., Ahmed, N. A., Yassen, N. N., & Zaki, H. F. (2018). The anti-inflammatory and anti-fibrotic effects of tadalafil in thioacetamide-induced liver fibrosis in rats. *Canadian Journal of Physiology and Pharmacology*, *96*(12), 1308–1317. https://doi.org/10.1139/cjpp-2018-0338

Miao, Y., Wu, Y., Jin, Y., Lei, M., Nan, J., & Wu, X. (2020). Benzoquinone derivatives with antioxidant activity inhibit activated hepatic stellate cells and attenuate liver fibrosis in TAA-induced mice. *Chemico-Biological Interactions*, *317*, 108945. https://doi.org/10.1016/j.cbi.2020.108945

Müller, A., Machnik, F., Zimmermann, T., & Schubert, H. (1988). Thioacetamide-induced cirrhosis-like liver lesions in rats usefulness and reliability of this animal model. *Exp Pathol*, *34*(4), 229–236. https://doi.org/10.1016/S0232-1513(88)80155-5

Palacios, R. S., Roderfeld, M., Hemmann, S., Rath, T., Atanasova, S., Tschuschner, A., Gressner, O. A., Weiskirchen, R., Graf, J., & Roeb, E. (2008). Activation of hepatic stellate cells is associated with cytokine expression in thioacetamide-induced hepatic fibrosis

in mice. *Laboratory Investigation*, *88*(11), 1192–1203. https://doi.org/10.1038/labinvest.2008.91

Panossian, A., Nikoyan, N., Ohanyan, N., Hovhannisyan, A., Abrahamyan, H., Gabrielyan, E., & Wikman, G. (2008). Comparative study of Rhodiola preparations on behavioral despair of rats. *Phytomedicine*, *15*, 84–91. https://doi.org/10.1016/j.phymed.2007.10.003

Placer, Z. A., Cushman, L. L., & Johnson, B. C. (1966). Estimation of product of lipid peroxidation (malonyldialdehyde) in biochemical systems. *Analytical Biochemistry*, *16*(2), 359–364.

Rio, D. C., Ares, M., Hannon, G. J., & Nilsen, T. W. (2010). Purification of RNA using TRIzol (TRI reagent). *Cold Spring Harbor, Protocols*, *6*, 1–3. https://doi.org/10.1101/pdb.prot5439

Roche, M., Dufour, C., Loonis, M., Reist, M., Carrupt, P. A., & Dangles, O. (2009). Olive phenols efficiently inhibit the oxidation of serum albumin-bound linoleic acid and butyrylcholine esterase. *Biochimica Et Biophysica Acta (BBA)-General Subjects*, *1790*(4), 240–248. https://doi.org/10.1016/j.bbagen.2009.01.007

Sambrook, J., Fritsch, E. F., & Maniatis, T. (1989). *Molecular cloning: A laboratory manual*. Cold Spring Harbor Laboratory Press.

Sánchez-Valle, V., Chavez-Tapia, N. C., Uribe, M., & Méndez-Sánchez, N. (2012). Role of oxidative stress and molecular changes in liver fibrosis: A review. *Current Medicinal Chemistry*, *19*(28), 4850–4860.

Sarna, L. K., Sid, V., Wang, P., Siow, Y. L., House, J. D., & Karmin, O. (2016). Tyrosol attenuates high fat diet-induced hepatic oxidative stress: Potential involvement of cystathionine β-synthase and cystathionine γ-lyase. *Lipids*, *51*(5), 583–590. https://doi.org/10.1007/s11745-015-4084-y

Sedlak, J., & Lindsay, R. H. (1968). Estimation of total, protein-bound, and nonprotein sulfhydryl groups in tissue with Ellman's reagent. *Analytical Biochemistry*, *25*, 192–205. https://doi.org/10.1016/0003-2697(68)90092-4

Sen, C. C., Yumusak, N., Faundez, R., Temamogullari, F., & Taskin, A. (2017). Evaluation of intra-testicular injections of calcium chloride and 4-vinylcyclohexene 1, 2 monoepoxide for chemical sterilization in guinea pigs. *Polish Journal of Veterinary Sciences*, *20*(2), 251–260. https://doi.org/10.1515/pjvs-2017-0030

Sharawy, M. H., El-Awady, M. S., & Makled, M. N. (2021). Protective effects of paclitaxel on thioacetamide-induced liver fibrosis in a rat model. *Journal of Biochemical and Molecular Toxicology*, *35*(5), e22745. https://doi.org/10.1002/jbt.22745

Smith, P. E., Krohn, R. I., Hermanson, G. T., Mallia, A. K., Gartner, F. H., Provenzano, M., & Klenk, D. C. (1985). Measurement of protein using bicinchoninic acid. *Analytical Biochemistry*, *150*(1), 76–85. https://doi.org/10.1016/0003-2697(85)90442-7

Stiuso, P., Bagarolo, M., Ilisso, C., Vanacore, D., Martino, E., Caraglia, M., Porcelli, M., & Cacciapuoti, G. (2016). Protective effect of tyrosol and S-adenosylmethionine against ethanol-induced oxidative stress of Hepg2 cells involves sirtuin 1, P53 and Erk1/2 signaling. *International Journal of Molecular Sciences*, *17*(5), 622. https://doi.org/10.3390/ijms17050622

Towbin, H., Staehelin, T., & Gordon, J. (1979). Electrophoretic transfer of proteins from polyacrylamide gels to nitrocellulose sheets: Procedure and some applications. *Proceedings of the National Academy of Sciences of the United States of America*; *76*(9): 4350–4354.

Trautwein, C., Friedman, S. L., Schuppan, D., & Pinzani, M. (2015). Hepatic fibrosis: Concept to treatment. *Journal of Hepatology*, *62*(1), S15–S24. https://doi.org/10.1016/j.jhep.2015.02.039

Wallace, M. C., Hamesch, K., Lunova, M., Kim, Y., Weiskirchen, R., Strnad, P., & Friedman, S. L. (2015). Standard operating procedures in experimental liver research: Thioacetamide model in mice and rats. *Laboratory Animals*, *49*(1), 21–29. https://doi.org/10.1177/0023677215573040

Yi, H. S., Eun, H. S., Lee, Y. S., Jung, J. Y., Park, S. H., Park, K. G., Choi, H. S., Suh, J. M., & Jeong, W. I. (2015). Treatment with 4-methylpyrazole modulated stellate cells and natural killer cells and ameliorated liver fibrosis in mice. *PLoS One*, *10*(5), e0127946. https://doi.org/10.1371/journal.pone.0127946

How to cite this article: Kutlu, T., Özkan, H., & Güvenç, M. (2021). Tyrosol retards induction of fibrosis in rats. *Journal of Food Biochemistry*, 45, e13965. https://doi.org/10.1111/jfbc.13965